

Complex-temperature properties of the 2D Ising model with $\beta H = \pm i\pi/2$

Victor Matveev† and Robert Shrock‡

Institute for Theoretical Physics, State University of New York, Stony Brook, NY 11794-3840, USA

Received 3 January 1995, in final form 25 May 1995

Abstract. We study the complex-temperature properties of a rare example of a statistical mechanical model which is exactly solvable in an external symmetry-breaking field, namely, the Ising model on the square lattice with $\beta H = \pm i\pi/2$. This model was solved by Lee and Yang. We first determine the complex-temperature phases and their boundaries. From a low-temperature, high-field series expansion of the partition function, we extract the low-temperature series for the susceptibility χ to $O(u^{23})$, where $u = e^{-4K}$. Analysing this series, we conclude that χ has divergent singularities (i) at $u = u_e = -(3 - 2^{3/2})$ with exponent $\gamma'_e = 5/4$, (ii) at $u = 1$, with exponent $\gamma'_1 = 5/2$, and (iii) at $u = u_s = -1$, with exponent $\gamma'_s = 1$. We also extract a shorter series for the staggered susceptibility and investigate its singularities. Using the exact result of Lee and Yang for the free energy, we calculate the specific heat and determine its complex-temperature singularities. We also carry this out for the uniform and staggered magnetization.

1. Introduction

The Ising model has long served as a prototype of a statistical mechanical system which undergoes a phase transition with associated spontaneous symmetry breaking and long range order. In the absence of an external magnetic field H , the free energy of the $d = 2$ (spin-1/2) Ising model was first calculated by Onsager [1], and the expression for the spontaneous magnetization first calculated by Yang [2], both for the square lattice. The model has never been solved in an arbitrary external magnetic field. However, in one of their classic papers, Lee and Yang [3] did succeed in solving exactly for the free energy and giving an exact expression for the magnetization of the Ising model on the square lattice for a particular manifold of values of H depending on the temperature T , given by

$$H = \frac{i\pi k_B T}{2}. \quad (1.1)$$

Although this is not a physical set of values, owing to the imaginary value of H and the resultant non-hermiticity of the Hamiltonian, this model is, nevertheless, of considerable interest as a rare example of a statistical mechanical model for which one has an exact solution in the presence of a symmetry-breaking field. Further work on the derivation of the Lee–Yang solution was reported in [4–7].

In the present paper, we shall investigate this model in a wider context, generalizing the temperature to complex values. There are several reasons for studying the properties of

† Email: vmatveev@max.physics.sunysb.edu

‡ Email: shrock@max.physics.sunysb.edu

statistical mechanical systems with the temperature variable generalized to take on complex values. First, one can understand more deeply the behaviour of various thermodynamic quantities by seeing how they behave as analytic functions of complex temperature. Second, one can see how the physical phases of a given model generalize to regions in appropriate complex-temperature variables. Third, a knowledge of the complex-temperature singularities of quantities which have not been calculated exactly helps in the search for exact, closed-form expressions for these quantities. This applies, in particular, to the susceptibility of the present model, which, like that of the zero-field Ising model, has never been calculated.

2. Generalities and complex-temperature phases

In this section we shall work out the complex-temperature phases and their boundaries. We begin with some definitions and notation. Recall that the Ising model is defined by the partition function $Z = \sum_{\{\sigma_n\}} e^{-\beta \mathcal{H}}$ with the Hamiltonian

$$\mathcal{H} = -J \sum_{\langle nn' \rangle} \sigma_n \sigma_{n'} - H \sum_n \sigma_n \quad (2.1)$$

where $\sigma_n = \pm 1$ are the Z_2 spin variables on each site n of the lattice, $\beta = (k_B T)^{-1}$, J is the exchange constant, $\langle nn' \rangle$ denote nearest-neighbour pairs and the units are defined such that the magnetic moment which would multiply the $H \sum_n \sigma_n$ is unity. We shall concentrate here on the square (sq) lattice. We use the standard notation $K = \beta J$, $h = \beta H$, $v = \tanh K$, $z = e^{-2K}$, $u = z^2 = e^{-4K}$, $w = 1/u$ and $\mu = e^{-2h}$. Note that v and z are related by the bilinear conformal transformation

$$z = \frac{1-v}{1+v}. \quad (2.2)$$

It will also be useful to introduce two elliptic moduli. The first is

$$\kappa = \frac{1}{C^2} = \frac{4u}{(1+u)^2} \quad (2.3)$$

which occurs in elliptic integrals in the exact expressions for the internal energy and specific heat, where we use the abbreviations

$$C \equiv \cosh(2K) \quad (2.4)$$

$$S \equiv \sinh(2K). \quad (2.5)$$

We record the symmetry

$$u \rightarrow 1/u \Rightarrow \kappa \rightarrow \kappa. \quad (2.6)$$

The second elliptic modulus,

$$k_{<} = \frac{i}{S(S^2 + 2)^{1/2}} = \frac{4iu}{(1-u)(1+6u+u^2)^{1/2}} \quad (2.7)$$

occurs in a natural way in the magnetization[†].

The reduced free energy per site is $f = -\beta F = \lim_{N_s \rightarrow \infty} N_s^{-1} \ln Z$ (where N_s denotes the number of sites on the lattice). In addition to the susceptibility itself, it will also be convenient to refer to the reduced susceptibility $\bar{\chi} = \beta^{-1} \chi$.

We begin by discussing the phase boundaries of the model as a function of complex temperature, i.e. the locus of points across which the free energy is non-analytic. As

[†] Note that these differ from the respective elliptic moduli κ_0 and $k_{<,0}$ which occur in the internal energy, specific heat and spontaneous magnetization for the Ising model on the square lattice at $h = 0$.

noted in [8], there is an infinite periodicity in complex K under the shift $K \rightarrow K + n i \pi$, where n is an integer, and, for lattices with even coordination number q , also the shift $K \rightarrow (2n + 1) i \pi / 2$, as a consequence of the fact that the spin-spin interaction $\sigma_i \sigma_j$ in \mathcal{H} is an integer. In particular, there is an infinite repetition of phases as functions of complex K ; these repeated phases are reduced to a single set by using the variables v, z or u (or variables based on these).

We also note an elementary symmetry involving h for the (spin-1/2) Ising model on a general lattice Λ . The low-temperature, high-field expansion of Z has the form

$$Z = e^{(q/2)N_s K} e^{N_s h} Z_r \tag{2.8}$$

where

$$Z_r = 1 + \sum_{n,m} a_{n,m}^{(\Lambda)} z^n \mu^m \tag{2.9}$$

where the only property of Z_r that we need is the fact that it is a polynomial in z and μ . In (2.8), we assume periodic boundary conditions, but for the free energy, in the thermodynamic limit, this is not essential. Now

$$h \rightarrow h + n i \pi \Rightarrow \mu \rightarrow \mu \tag{2.10}$$

where n is an integer. Hence, under such a shift, the only change in Z is in the prefactor, $e^{N_s h}$. Equivalently, in the corresponding (reduced) free energy

$$f = (q/2)K + h + \lim_{N_s \rightarrow \infty} N_s^{-1} \left(1 + \sum_{n,m} a_{nm}^{(\Lambda)} z^n \mu^m \right) \tag{2.11}$$

the only change is in the second term, h . Therefore, aside from this term, one may, and we shall, restrict to the range

$$-\frac{i\pi}{2} < \text{Im}(h) \leq \frac{i\pi}{2} \tag{2.12}$$

without loss of generality. In the present context, we shall consider just the value $h = i\pi/2$; our results will apply in the same way to $h = -i\pi/2$.

It is useful to review the connection between the square-lattice Ising model with $h = i\pi/2$ and the Ising model on the square lattice in zero field [6, 7]. This is done by first considering the Ising model on the checkerboard (also called generalized square) lattice, defined by assigning different couplings $K_j, j = 1, \dots, 4$, to the bonds of the square lattice, as shown in figure 1. Again, for discussions of the partition function, we assume periodic boundary conditions. The free energy [9] and spontaneous magnetization [10, 11] are known for the zero-field checkerboard Ising model. Now recall the identity

$$e^{h\sigma} = \cosh h + \sigma \sinh h \tag{2.13}$$

for $\sigma = \pm 1$. For $h = i\pi/2$, this reduces to $e^{h\sigma_n} = i\sigma_n$, and hence $\exp(h \sum_n \sigma_n) = \prod_n (i\sigma_n)$.

Next, consider a dimer site covering of the checkerboard lattice, where by site covering, we mean that each site is the member of one (and only one) dimer. As is clear from figure 1, a simple covering of this sort is provided by each of the bonds of a single type, say those with the K_4 couplings. We may thus associate pairs of the σ_n s in the above product with the dimers of this covering. To do this, we separate one of the two factors of i for such pair and place it in front of Z . One then has

$$Z_{\text{ch}} = i^{N_s/2} \sum_{\{\sigma_n\}} \left(\prod_{(rs)} (i\sigma_r \sigma_s) \right) \exp \left(\sum_{\langle n,n' \rangle} \sigma_n K_{nn'} \sigma_{n'} \right) \tag{2.14}$$

where ch denotes checkerboard and $K_{nn'}$ refers to the appropriate K_j , $j = 1-4$ depending on which bond connects the sites n and n' (cf figure 1). Then one can use the identity (2.13) again to write

$$Z = i^{N_s/2} \sum_{\{\sigma_n\}} \exp \left(\sum_{\langle nn' \rangle} \sigma_n K'_{nn'} \sigma_{n'} \right) \tag{2.15}$$

that is,

$$Z(\{K_i\}; h = i\pi/2)_{\text{ch}} = (i)^{N_s/2} Z(\{K'_i\}; h = 0)_{\text{ch}} \tag{2.16}$$

where $K'_i = K_i$, $i = 1, 2, 3$, and

$$K'_4 = K_4 + \frac{i\pi}{2}. \tag{2.17}$$

Hence, for the free energy,

$$f(\{K_i\}; h = i\pi/2)_{\text{ch}} = \frac{i\pi}{4} + f(\{K'_i\}; h = 0)_{\text{ch}}. \tag{2.18}$$

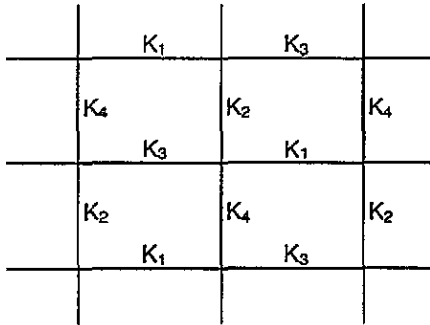


Figure 1. Assignment of couplings K_i , $i = 1-4$ to links (bonds) of the checkerboard lattice.

Then, setting $K_i = K$, $i = 1, 2, 3, 4$, one can obtain the Lee–Yang result for $f(K, h = i\pi/2)$ [3] from the (analytic continuation of the) free energy for the zero-field checkerboard lattice [9]. The same method works for the magnetization and yields the relation

$$M(\{K_i\}, h = i\pi/2)_{\text{ch}} = M(\{K'_i\}, h = 0)_{\text{ch}} \tag{2.19}$$

and the m -point correlation functions satisfy

$$\langle \sigma_{n_1} \dots \sigma_{n_m} \rangle (\{K_i\}, h = i\pi/2)_{\text{ch}} = \langle \sigma_{n_1} \dots \sigma_{n_m} \rangle (\{K'_i\}, h = 0)_{\text{ch}}. \tag{2.20}$$

Further, it follows from the special case of (2.20) for two-spin correlation functions, together with the expression for the susceptibility as a sum over the connected (conn) two-spin correlation functions

$$\bar{\chi} = \sum_r \langle \sigma_0 \sigma_r \rangle_{\text{conn}} \tag{2.21}$$

where $\langle \sigma_0 \sigma_r \rangle_{\text{conn}} \equiv \langle \sigma_0 \sigma_r \rangle - M^2$, that

$$\bar{\chi}(\{K_i\}, h = i\pi/2)_{\text{ch}} = \bar{\chi}(\{K'_i\}, h = 0)_{\text{ch}}. \tag{2.22}$$

Of course, the Ising model with zero field is not equivalent to one with non-zero field, since in the former case the partition function and free energy are exactly invariant under the Z_2

transformation $\sigma_n \rightarrow -\sigma_n$, whereas in the latter case this symmetry is broken explicitly by the external field term. This inequivalence is manifested in the fact that equations (2.16)–(2.17) are not Z_2 -invariant. Thus under the transformation $\sigma_n \rightarrow -\sigma_n$, which is equivalent to $h \rightarrow -h$, the i 's in these equations are replaced by $-i$. It is also manifested in the fact that while the zero-field Ising model always has a Z_2 -symmetric paramagnetic (PM) phase, the model with non-zero external field $h \neq 0$ does not have any PM phase. The usefulness of equation (2.18) stems from the special feature that for $h = \pm i\pi/2$, this non-invariance is localized to just a constant term in the free energy. The square-lattice Ising model with $h = i\pi/2$ is also related to a certain frustrated Ising model [12].

The (reduced) free energy is [3]†

$$f(K, h = \pm i\pi/2) = \pm \frac{i\pi}{2} + \ln 2 + \frac{1}{4} \int_{-\pi}^{\pi} \int_{-\pi}^{\pi} \frac{d\theta_1 d\theta_2}{(2\pi)^2} \times \ln \left\{ \frac{1}{2} [C^4 + S^4 - 1 + S^2 (\cos(\theta_1 + \theta_2) - \cos(\theta_1 - \theta_2))] \right\} \quad (2.23)$$

where C and S were defined in (2.4) and (2.5). From $U = -\partial f / \partial \beta = -J \partial f / \partial K$, one has the symmetries

$$U \left(\beta, J, H = \frac{i\pi}{2\beta} \right) = U \left(\beta, J, H = -\frac{i\pi}{2\beta} \right) \quad (2.24)$$

$$U \left(\beta, -J, h = \frac{i\pi}{2} \right) = U \left(\beta, J, h = \frac{i\pi}{2} \right) \quad (2.25)$$

$$U \left(-\beta, J, h = \frac{i\pi}{2} \right) = -U \left(\beta, J, h = \frac{i\pi}{2} \right). \quad (2.26)$$

Similarly, from $C = k_B K^2 \partial^2 f / \partial K^2$, one has

$$C \left(K, h = \frac{i\pi}{2} \right) = C \left(K, h = -\frac{i\pi}{2} \right) \quad (2.27)$$

and

$$C \left(K, h = \frac{i\pi}{2} \right) = C \left(-K, h = \frac{i\pi}{2} \right). \quad (2.28)$$

The free energy is trivially divergent at $K = \pm\infty$, i.e. $u = 0, \infty$; however, this will not be important here since these are isolated points and not part of any phase boundaries. The curves along which the free energy is non-analytic are given by the locus of points where the argument of the logarithm in the integrand of equation (2.23) vanishes. Expressed in terms of the variable u , f is

$$f(K, h = \pm i\pi/2) = \pm \frac{i\pi}{2} + \frac{1}{4} \ln \left[\frac{(1-u)^2}{u^2} \right] + \frac{1}{4} \int_{-\pi}^{\pi} \int_{-\pi}^{\pi} \frac{d\theta_1 d\theta_2}{(2\pi)^2} \ln [(1+u)^2 - 2uP(\theta_1, \theta_2)] \quad (2.29)$$

where

$$P(\theta_1, \theta_2) = \cos \theta_1 + \cos \theta_2. \quad (2.30)$$

† The Hamiltonian in [3] was defined with a different zero point of the energy than that used here.

The above locus of points where the argument of the logarithm vanishes is given by the solutions of the equation

$$(1 + u)^2 - 2ux = 0 \quad (2.31)$$

where $x = P(\theta_1, \theta_2)$, taking values in the range $-2 \leq x \leq 2$. These are integrable singularities. Since the coefficients in this equation are real, the solutions are either real or consist of complex conjugate pairs. Moreover, under the replacement $u \rightarrow 1/u$, equation (2.31) retains its form, up to an overall factor of u^{-2} . Consequently, the locus of solutions is also invariant under this mapping $u \rightarrow 1/u$. The solutions are shown in figure 2(a) and consist of the union of the unit circle

$$u = e^{i\phi} \quad -\pi < \phi \leq \pi \quad (2.32)$$

and the finite line segment

$$\frac{1}{u_e} \leq u \leq u_e \quad (2.33)$$

where the inner endpoint is

$$u_e = -(3 - 2\sqrt{2}) = -0.171\,572\,875 \dots \quad (2.34)$$

and the outer endpoint is $1/u_e = -(3 + 2\sqrt{2}) = -5.828\,427 \dots$. Note that $u_e = -u_c$, where u_c is the usual critical point in the zero-field square lattice Ising model separating the Z_2 -symmetric, paramagnetic (PM) phase from the phase in the Z_2 symmetry is spontaneously broken by long-range ferromagnetic (FM) long-range order.

It is of interest to see how the solutions to equation (2.31) are traced out in the complex u plane as x varies. For $x = 2$, this equation has a double root at $u = 1$. As x decreases from two to zero, this root splits into a complex conjugate pair, the members of which move counterclockwise and clockwise along the unit circle, and finally rejoin to form a double root at $u = -1$ when $x = 0$. As x decreases from zero to -2 , this double root again splits, but this time into two reciprocal real roots, one of which moves to the right, from $u = -1$ to the endpoint u_e and the other of which moves leftward to $u = 1/u_e$. The corresponding phase boundaries in the z plane consist of the unit circle $|z| = 1$ together with the two line segments from $z = \pm u_e = \pm i(\sqrt{2} - 1)$ upward and downward along the imaginary axis to $z = \mp 1/u_e = \pm i(\sqrt{2} + 1)$, respectively.

The circle (2.32) divides the u plane into two separate phases. A fundamental property of this model is that the non-zero external field breaks the Z_2 symmetry explicitly, so that there is no Z_2 -symmetric phase. Even without using the known expression for the magnetization, one can identify the phases in this diagram as follows. For sufficiently large real K , the interaction of the external magnetic field with the spins is negligible compared with the spin-spin interaction, which thus produces a ferromagnetically ordered phase, just as it does in the model with $h = 0$. This shows that the neighbourhood of the origin in the u (or z) plane is ferromagnetically ordered. By analytic continuation, it then follows that the entire region inside the unit circle $|u| = 1$ is a ferromagnetically ordered phase, and this is so denoted in figure 2(a). Similarly, for sufficiently large negative K , the interaction of the external field with the spins is again negligible compared with the spin-spin interaction, which produces a phase with antiferromagnetic (AFM) long-range order. By analogous analytic continuation arguments, it follows that the entire region outside the unit circle is the AFM phase. In passing, we note that complex-temperature properties of the $h = 0$ Ising model on $d = 2$ lattices have been studied in [8, 13–21]. In the case $h = 0$ for the square lattice, the analogous locus of points, across which the free energy is singular, form a limaçon [20] defined by $\text{Re}(u) = 1 + 2^{3/2} \cos \omega + 2 \cos 2\omega$, $\text{Im}(u) = 2^{3/2} \sin \omega + 2 \sin 2\omega$

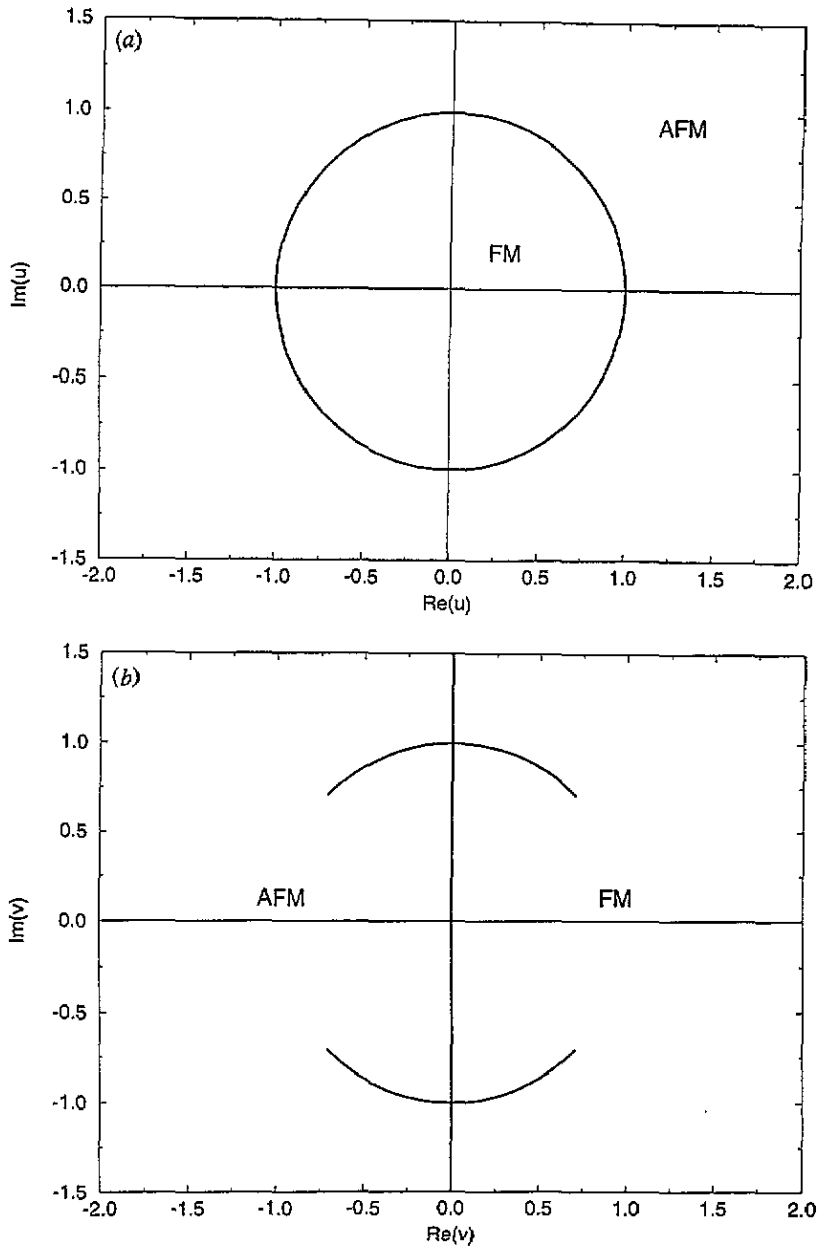


Figure 2. (a) Phases and associated boundaries in the complex u plane for the Ising model on the square lattice with $h = \pm i\pi/2$. The boundaries are given by equations (2.32) and (2.33) in the text. In particular, the line segment extends from u_e as given in equation (2.34) off the figure to the left, ending at $1/u_e = -(3 + 2\sqrt{2}) \simeq -5.828$. FM and AFM refer to phases in which $M \neq 0, M_{SI} = 0$ and $M = 0, M_{SI} \neq 0$, respectively. (b) The complex-temperature phase diagram in the v plane.

for $0 \leq \omega < 2\pi$, or equivalently, in the z plane, the circles [13, 14] $z = \pm 1 + \sqrt{2}e^{i\theta}$, for $0 \leq \theta < 2\pi$.

By the use of the conformal mapping (2.2) on the z plane, or by re-expressing the free energy in terms of the variable v and again solving for the locus of points where the argument of the logarithm vanishes, we find that the phase diagram of the model in the v plane is as shown in figure 2(b). The unit circle $|z| = 1$ is mapped to the imaginary axis in the v plane, and the respective line segments from $z = \pm z_c$ to $\mp 1/z_c$ are mapped to the arcs from $v = e^{\mp i\pi/4}$ to $v = e^{\mp 3i\pi/4}$. It is interesting that the $\text{Re}(v) = 0$ (i.e. imaginary) axis forms the boundary between the complex-temperature FM and AFM phases. One may understand this by recalling that: (i) if h were real and positive (negative), this would favour FM (AFM) ordering, but a pure imaginary value of h does not favour FM over AFM ordering, or *vice versa*; (ii) similarly, if the spin-spin coupling K is real and positive (negative), it favours FM (AFM) ordering, but a pure imaginary value of K (and hence v) does not favour FM over AFM ordering, or *vice versa*. Therefore, if both h and K are pure imaginary, as is the case here for the imaginary axis in the v plane, then the system is precisely balanced between FM and AFM order, so that this axis should be the boundary between the complex-temperature FM and AFM phases, and this is just what our explicit calculation shows.

The mapping defined by $u \rightarrow \kappa^2$, where κ was defined in (2.3), takes the the locus of points (2.32) and (2.33) to a single semi-infinite line segment extending from 1 to ∞ in the complex κ^2 plane. All points in the κ^2 plane are analytically connected to all other points. In particular, the mapping $u \rightarrow \kappa^2$ takes both the complex-temperature FM and AFM phases in the u plane to the same respective regions in the κ^2 plane, as is clear from the symmetry (2.6) and the fact that the transformation $u \rightarrow 1/u$ interchanges the FM and AFM phases in the u plane.

3. Complex-temperature behaviour of the internal energy and specific heat

3.1. Exact expressions

From the free energy (2.29), it is straightforward to calculate the internal energy U and specific heat C (per site). In terms of the variable u , we find that

$$U = -J \left[\frac{1+u}{1-u} + \left(\frac{1-u}{1+u} \right) \left(\frac{2}{\pi} \right) K(\kappa) \right] \quad (3.1)$$

where the elliptic modulus κ was given above in equation (2.3) and $K(k) = \int_0^{\pi/2} (1 - k^2 \sin^2 \theta)^{-1/2} d\theta$ is the complete elliptic integral of the first kind. This expression holds for both the FM and AFM phases and exhibits the symmetries (2.25) and (2.26). Since either of these has the effect of taking $u \rightarrow 1/u$, and since this mapping takes the interior of the complex-temperature FM phase to the interior of the complex-temperature AFM phase, the values of U in these two phases are simply related by (2.25)–(2.26). In the FM phase, the first few terms of the small- $|u|$ expansion (complex-temperature generalization of the low-temperature expansion) are

$$U = -2J[1 + 4u^2 - 12u^3 + 60u^4 - 280u^5 + O(u^6)]. \quad (3.2)$$

In the AFM phase, the corresponding expansion parameter is $w = 1/u$, and U has the same expansion as (3.2) with J replaced by $-J$ and u replaced by w .

As discussed above, in the limit $J \rightarrow \infty$, and hence $K \rightarrow \infty$ with fixed H , the spin-spin interaction overwhelms the contribution of the external field coupling, which therefore has a negligible effect, to leading order. It follows that in this limit, the value of the internal energy should be the same as the value for $h = 0$, i.e.

$$U(u = 0, h = i\pi/2) = U(u = 0, h = 0). \quad (3.3)$$

It is interesting to compare the small- $|u|$ series expansions of these two functions to ascertain the finite- u corrections to this equality. For this purpose, we recall that [1]

$$U(K, h = 0) = -J \left[\frac{1+u}{1-u} + \frac{(1-6u+u^2)}{(1-u^2)} \left(\frac{2}{\pi} \right) K(\kappa_0) \right] \quad (3.4)$$

where

$$\kappa_0 = \frac{4z(1-u)}{(1+u)^2}. \quad (3.5)$$

The expression (3.4) holds for all phases, PM, FM and AFM. In the FM phase, it has the small- $|u|$ expansion

$$U(h = 0) = -2J[1 - 4u^2 - 12u^3 - 36u^4 - 120u^5 + O(u^6)]. \quad (3.6)$$

Clearly, the expansions (3.2) and (3.6) agree with the relation (3.3) for $u = 0$. $U(K, h = 0)$ also satisfies the symmetries analogous to (2.25) and (2.26), with $h = i\pi/2$ replaced by $h = 0$; as a consequence, in the AFM phase, the small- $|w|$ expansion of $U(K, h = 0)$ is given by (3.6) with J replaced by $-J$ and u replaced by w .

For C we get

$$\frac{C}{8k_B K^2} = -\frac{u}{(1-u)^2} - \frac{(1+u)^2}{\pi(1+6u+u^2)} E(\kappa) + \frac{(1+u^2)}{\pi(1+u)^2} K(\kappa) \quad (3.7)$$

where $K(k)$ was defined above and $E(k) = \int_0^{\pi/2} (1-k^2 \sin^2 \theta)^{1/2} d\theta$ is the complete elliptic integral of the second kind. Again, this expression holds for both the FM and AFM phases. It will also be useful to express C in an equivalent form, using (2.3)

$$\frac{C}{8k_B K^2} = -\frac{u}{(1-u)^2} - \frac{E(\kappa)}{\pi(1+\kappa)} + \frac{(1+u^2)(1+\kappa)K(\kappa)}{\pi(1+6u+u^2)}. \quad (3.8)$$

C/K^2 has the small- $|u|$ expansion

$$\frac{C}{8k_B K^2} = -64u^2 + 288u^3 - 1920u^4 + 11200u^5 + O(u^6). \quad (3.9)$$

For comparison, the specific heat for the Ising model on the square lattice with $h = 0$ [1] is

$$\frac{C}{k_B K^2} = \frac{4(1-\kappa')}{\pi\kappa^2} \left[2\{K(\kappa_0) - E(\kappa_0)\} - (1-\kappa'_0) \left\{ \frac{\pi}{2} + \kappa'_0 K(\kappa_0) \right\} \right] \quad (3.10)$$

which has the small- $|u|$ expansion

$$\frac{C}{k_B K^2} = 64u^2 + 288u^3 + 1152u^4 + 4800u^5 + O(u^6). \quad (3.11)$$

Of course, in this case, the positivity of the specific heat requires that the coefficient of the lowest order term must be positive (the first negative coefficient occurs in the u^7 term). We proceed to determine the complex-temperature singularities of U and C for the present case, $h = i\pi/2$.

3.2. Vicinity of $u = u_e$

As discussed in connection with figure 2(a), the point $u = u_e$ is the endpoint of the singular line segment protruding into the complex-temperature extension of the FM phase. All approaches to this point, except directly from the left along this singular line segment,

occur from within the complex-temperature FM phase. As $u \rightarrow u_e = -(3 - 2^{3/2})$, $\kappa \rightarrow -1$. The internal energy diverges like

$$\frac{U}{J} \rightarrow \frac{\sqrt{2}}{\pi} \ln(1 - u/u_e) \quad \text{as } u \rightarrow u_e. \quad (3.12)$$

In the specific heat, the dominant divergence arises from the term in (3.7) involving $E(\kappa)$ and is

$$\frac{C}{k_B K^2} \rightarrow -\frac{4\sqrt{2}}{\pi(1 - u/u_e)} \quad \text{as } u \rightarrow u_e \quad (3.13)$$

so that the associated singular exponent for C at $u = u_e$ is

$$\alpha'_{e,\text{FM}} \equiv \alpha'_e = 1 \quad (3.14)$$

where the subscript FM indicates the phase from which this point is approached, and the prime is the standard notation indicating that the approach to this singular point is from within a broken-symmetry phase. (The last feature is, of course, true of all of the singular points for $h \neq 0$.) There is also a weaker, logarithmic divergence arising from the term involving $K(\kappa)$. The value of K at u_e in (3.13) is

$$K_e = -\frac{1}{4} \ln u_e = -\frac{1}{4} [\ln(3 - 2^{3/2}) + i\pi + 2n\pi] \quad (3.15)$$

where n labels the Riemann sheet used for the evaluation of the logarithm, which we shall take to be $n = 0$ below, unless otherwise indicated.

3.3. Vicinity of $u = 1/u_e$

The point $u = 1/u_e$ is the left end of the singular line segment protruding into the complex-temperature extension of the AFM phase. Except for the approach directly from the right along the singular line segment, all approaches to this point occur from within the complex-temperature AFM phase. As $u \rightarrow 1/u_e$, $\kappa \rightarrow -1$, as is clear from the previous remarks and the symmetry (2.6). The internal energy again diverges like

$$\frac{U}{J} \rightarrow -\frac{\sqrt{2}}{\pi} \ln(1 - u_e u) \quad \text{as } u \rightarrow \frac{1}{u_e}. \quad (3.16)$$

In the specific heat, the dominant divergence again arises from the term in (3.7) involving $E(\kappa)$ and is

$$\frac{C}{k_B K^2} \rightarrow \frac{4\sqrt{2}}{\pi(1 - u_e u)} \quad \text{as } u \rightarrow 1/u_e \quad (3.17)$$

so that the associated singular exponent for C at the outer endpoint (oe) $u = 1/u_e$ is

$$\alpha'_{\text{oe,AFM}} \equiv \alpha'_{\text{oe}} = 1. \quad (3.18)$$

The value of K corresponding to $u = 1/u_e$ in equation (3.17) is, for the principal Riemann sheet of the log, $K_{\text{oe}} = -(1/4)[\ln(3 + 2^{3/2}) + i\pi]$.

3.4. Vicinity of $u = -1$

As $u \rightarrow -1$ (denoted u_s), κ diverges; if we set $u = -1 + \epsilon e^{i\phi}$ and let $\epsilon \rightarrow 0$, then $\kappa \sim -4\epsilon^{-2} e^{-2i\phi}$. One easily sees that $U(u = -1)$ is finite. For C , we observe that the first and second terms on the right-hand side of equation (3.7) or (3.8) are finite. By the use

of the elliptic integral identity $(1 + \kappa)K(\kappa) = K(2\kappa^{1/2}/(1 + \kappa))$ (see, e.g. [22]), we can rewrite the term involving $K(\kappa)$ in equation (3.8) as

$$\frac{(1 + u^2)}{\pi(1 + 6u + u^2)} K\left(\frac{2\kappa^{1/2}}{1 + \kappa}\right). \tag{3.19}$$

As $u \rightarrow -1$ and κ diverges, $K(2\kappa^{1/2}/(1 + \kappa)) \rightarrow K(0) = \pi/2$, so that C is finite, although non-analytic, at $u = -1$. This is true for the approach to $u = -1$ from either the FM or AFM phases. We thus have

$$\alpha'_{s,FM} = \alpha'_{s,AFM} = 0 \quad (\text{log finite}). \tag{3.20}$$

3.5. Vicinity of $u = 1$

As $u \rightarrow 1$, $\kappa \rightarrow 1$. In U the leading potential singularity arises from the first term in (3.1)

$$\frac{U}{J} \rightarrow \frac{-2}{1 - u} \quad \text{as } u \rightarrow 1. \tag{3.21}$$

Now $K = -(1/4) \ln u$, so that, if one uses the first Riemann sheet of the logarithm, then $u \rightarrow 1$ maps to $K \rightarrow 0$. Recalling that $K = \beta J$, if this zero in K is due to $\beta \rightarrow 0$ at fixed non-zero J , then equation (3.21) shows that U diverges for $u \rightarrow 1$; however, if the zero in K is due to $J \rightarrow 0$ at fixed non-zero β , then, expanding (3.21), one finds that $U \rightarrow 1/(2\beta)$.

For the specific heat, from (3.7), it follows that as $u \rightarrow 1$

$$k_B^{-1}C \rightarrow 8K^2 \left[-\frac{1}{(1 - u)^2} + \frac{1}{4\pi} \ln\left(\frac{32}{(1 - u)^2}\right) + \dots \right] \tag{3.22}$$

where ... refers to less singular terms. If we again use the principal Riemann sheet of the logarithm, so that $u \rightarrow 1$ corresponds to $K \rightarrow 0$, then (3.22) becomes

$$k_B^{-1}C \rightarrow -\frac{1}{2} + \frac{2}{\pi} K^2 \ln\left(\frac{2}{K^2}\right) + O(K^2) \quad \text{as } u \rightarrow 1. \tag{3.23}$$

That is, C has a finite logarithmic singularity at this point, and hence a corresponding exponent

$$\alpha'_{1,FM} = \alpha'_{1,AFM} = 0 \quad (\text{log finite}). \tag{3.24}$$

In passing, we note that if one were to use a Riemann sheet different from the principal ($n = 0$) one in evaluating $K = -(1/4) \ln(1)$, so that $K = -in\pi/2 \neq 0$, then C would diverge quadratically at $u = 1$.

3.6. Elsewhere along the singular curves

We discuss here the behaviour of U and C as one crosses the singular locus of points comprised by the unit circle (2.32) and the line segment (2.33) away from the points $u = u_e$, $1/u_e$, -1 and 1 . The singularities which one encounters in this case are associated with passage across the branch cut of the elliptic integrals in (3.1) and (3.7). We recall that the elliptic integrals $K(\kappa)$ and $E(\kappa)$ are analytic functions of κ^2 in the complex κ^2 plane except for respectively divergent and finite branch points at $\kappa^2 = 1$ and an associated branch cut, which is normally taken to run from $\kappa^2 = 1$ to $\kappa^2 = \infty$ along the positive real axis in this plane. To illustrate the nature of the singularities, we shall consider moving outward along a ray in the u plane defined by $u = \rho e^{i\theta}$ with ρ increasing from 0 to ∞ at fixed θ , say $\theta = \pi/6$. As shown in figure 3, the image point in the κ^2 plane also moves out from the origin, starting with an angle of $\pi/3$ but bending around to the right. As we cross the unit

circle in the u plane, leaving the FM phase and entering the AFM phase, the image point in the κ^2 plane crosses the branch cut moving vertically downward. This branch cut is precisely the image of the unit circle $|u| = 1$ (and also of the singular line segment (2.33)). For $\theta = \pi/6$, the crossing point is at $\kappa^2 = 2^4(7 - 4\sqrt{3}) = 1.1487\dots$ In the κ^2 plane, one thus passes onto the second Riemann sheet of the elliptic functions $K(\kappa)$ and $E(\kappa)$. If one projects back to the first Riemann sheet, these functions have discontinuous imaginary parts across this branch cut. As ρ continues to increase toward ∞ , $\kappa^2 \sim 16\rho^{-2}e^{-2\theta}$ so that the image point curves around and finally approaches the origin in a 'northwest' direction, at an angle of $-\pi/3$, but on the second Riemann sheet. In figure 3 we show the image point for ρ in the range from zero to 30.

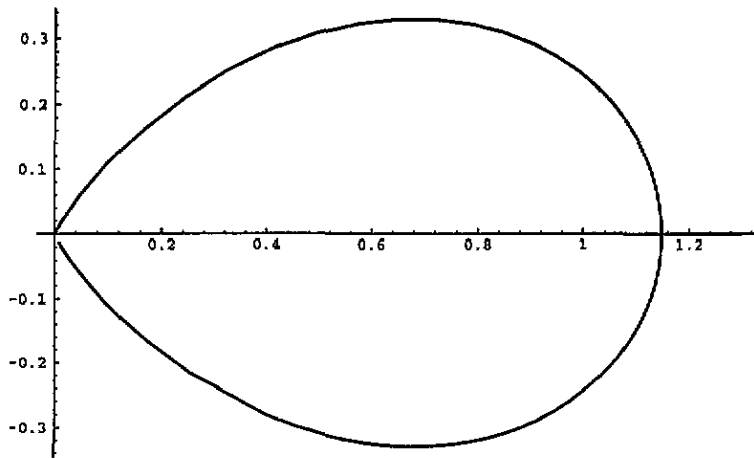


Figure 3. The path of κ^2 corresponding to $u = \rho e^{i\theta}$ for $\theta = \pi/6$, as ρ varies from 0 to 30. Horizontal and vertical axes are the $\text{Re}(\kappa^2)$ and $\text{Im}(\kappa^2)$ axes. The image of the singular curve (2.32) and line segment (2.33) is the dark line from $\kappa^2 = 1$ to $\kappa^2 = \infty$.

4. Complex-temperature behaviour of the uniform and staggered magnetization

The magnetization M is [3, 5]

$$M(u, h = i\pi/2) = \frac{(1+u)^{1/2}}{(1-u)^{1/4}(1+6u+u^2)^{1/8}}. \quad (4.1)$$

Note that $(1+6u+u^2) = (1-u/u_c)(1-u_c u)$. By analytic continuation, this formula holds throughout the complex-temperature extension of the FM phase. The identity discussed above, and the resultant equation (2.19) yields the relation

$$M(u, h = \pm i\pi/2) = M(-u, h = 0)^{-1} \quad (4.2)$$

where [2]

$$M(u, h = 0) = \frac{(1+u)^{1/4}(1-6u+u^2)^{1/8}}{(1-u)^{1/2}}. \quad (4.3)$$

As is well known, one can express $M(u, h = 0)$ as

$$M(u, h = 0) = (1 - (k_{z,0})^2)^{1/8} \quad (4.4)$$

where

$$k_{<,0} = \frac{1}{\sinh^2(2K)} = \frac{4u}{(1-u)^2} \tag{4.5}$$

This quantity also enters in exact expressions for correlation functions in the FM phase of the $h = 0$ Ising model [23–25]. Given the relation (4.2), it is natural to write

$$M(u, h = i\pi/2) = (1 - (k_{<})^2)^{1/8} \tag{4.6}$$

where the elliptic modulus was introduced in equation (2.7). The magnetization for the $h = i\pi/2$ case vanishes continuously at the point $u = -1$ (denoted u_s) with exponent

$$\beta_s = \frac{1}{2} \tag{4.7}$$

diverges at $u = u_e$ with exponent

$$\beta_e = -\frac{1}{8} \tag{4.8}$$

and diverges at $u = 1$ with exponent

$$\beta_1 = -\frac{1}{4} \tag{4.9}$$

Elsewhere on the boundary of the complex-temperature extension of the FM phase, i.e. the unit circle in the u plane, M vanishes discontinuously. Note that the apparent divergence at the point $u = 1/u_e$ does not actually occur, since this is outside of the complex-temperature FM phase, where the above analytic continuation is valid.

The staggered magnetization M_{st} does not seem to have been explicitly discussed in the literature, but one can easily obtain it, as follows. M_{st} may be defined via

$$M_{st}^2 = \lim_{|r| \rightarrow \infty} (\bar{\sigma}_0 \bar{\sigma}_r) \tag{4.10}$$

where

$$\bar{\sigma}_r = (-1)^{p(r)} \sigma_r \tag{4.11}$$

where

$$p(\mathbf{r}) = \sum_{i=1}^2 r_i \tag{4.12}$$

i.e. $\bar{\sigma}_r = \sigma_r$ for \mathbf{r} on the same sublattice as $\mathbf{r} = \mathbf{0}$ and $-\sigma_r$ for \mathbf{r} on the other sublattice of the (bipartite) square lattice. To evaluate M_{st} via equation (4.10), it suffices to take $\mathbf{r} = (r, 0)$ or $(0, r)$, i.e. the row or column two-spin correlation function. From the known asymptotic behaviour of this correlation function [5], one immediately finds that

$$M_{st}(w) = M(u \rightarrow w) \tag{4.13}$$

where, as before, $w = 1/u$. This is consistent with equation (4.6) since (cf (2.6)) $u \rightarrow 1/u$ takes $k_{<} \rightarrow -k_{<}$, and $k_{<}$ enters squared in (4.6). Of course, M_{st} vanishes identically outside the complex-temperature extension of the AFM phase. Further, we may immediately conclude that M_{st} vanishes continuously at $u = -1$ with exponent (4.7), diverges at $u = 1/u_e$ with exponent (4.8), and diverges at $u = 1$ with exponent (4.9). Elsewhere along the boundary of the complex-temperature AFM phase, M_{st} vanishes discontinuously, with the same discontinuity as M .

It is of interest to compare these results with the behaviour of M and M_{st} for $h = 0$ (again on the square lattice). Aside from the physical PM–FM and PM–AFM critical points $u = u_c = (3 - 2^{3/2})$ and $1/u_c$, where, respectively, M and M_{st} vanish continuously with exponent $\beta = 1/8$, they also both vanish continuously at the complex-temperature point $u = -1$, with the same exponent, $\beta = 1/4$. Note that for $h = 0$ there is only one point, viz., $u = -1$, where the FM and AFM phases are contiguous and M and M_{st} vanish continuously, whereas for $h = i\pi/2$ there are two such points, namely, $u = -1$ and $u = 1$.

5. Extraction and analysis of the low-temperature series for $\bar{\chi}$

5.1. Generalities

In order to investigate the complex-temperature singularities of the susceptibility $\bar{\chi}$, we shall make use of the low-temperature, high-field series expansion for the free energy or equivalently the partition function of the Ising model on the square lattice [26–28]. In [28], Baxter and Enting calculated this expansion for the partition function to order $O(u^{23})$. The series for Z_r in equation (2.9) is

$$Z_r = 1 + \sum_{n=2}^{\infty} \sum_m a_{n,m} u^n \mu^m \quad (5.1)$$

where $j \leq m \leq j^2$ for $n = 2j$ and $j \leq m \leq j(j-1)$ for $n = 2j-1$. We extract the series for $h = i\pi/2$ by calculating $\bar{\chi} = \partial^2 f / \partial h^2$ and then substituting $\mu = -1$. This has the form

$$\bar{\chi}(u, h = i\pi/2) = 4u^2 \left(\sum_{n=0}^{\infty} c_n u^n \right). \quad (5.2)$$

The results for the c_n are listed in table 1; the series for Z and the resultant series for $\bar{\chi}$ to $O(u^{23})$ yields the c_n s to order $n = 21$. Parenthetically, we note that $\bar{\chi}$ has been calculated to $O(u^{28})$ in [29] and to $O(u^{38})$ in [18], but the low-temperature, high-field expansion of the partition function as a function of $\mu = e^{-2h}$, which would be necessary to extract $\bar{\chi}(h = i\pi/2)$, was not given in these papers (it would be a rather long expression).

Table 1. Low-temperature series expansion coefficients for $\bar{\chi}(u, h = i\pi/2)$ in equation (5.2).

n	c_n
0	-1
1	8
2	-48
3	304
4	-1863
5	11 368
6	-68 840
7	414 872
8	-2 490 437
9	14 903 648
10	-88 963 696
11	529 939 176
12	-3 151 205 475
13	18 710 180 192
14	-110 948 037 424
15	657 164 715 520
16	-3 888 670 886 593
17	22 990 566 432 904
18	-135 819 110 416 784
19	801 806 651 588 848
20	-4 730 485 389 238 263
21	27 892 958 533 539 784

We have analysed this series using dlog Padé and differential approximants. For a recent review of these techniques, see [30]. Our notation for these approximants follows [30] and our earlier work on complex-temperature properties of the $h = 0$ Ising model [19–21]. In

particular, we use first-order differential approximants (i.e. $K = 1$ in our previous notation); as before, we used unbiased approximants so as to be able to use an extrapolation method for extracting critical exponents. Since the prefactor $4u^2$ is analytic, we have actually performed the analysis on the reduced function

$$\bar{\chi}_r \equiv \frac{\bar{\chi}}{4u^2} = \sum_{n=0}^{\infty} c_n u^n. \quad (5.3)$$

As one approaches a generic complex singular point denoted sing from within the complex-temperature extension of the FM phase,

$\bar{\chi}$ is assumed to have the leading singularity

$$\bar{\chi} \sim A'_{\text{sing}} (1 - u/u_{\text{sing}})^{-\gamma'_{\text{sing}}} (1 + a_1(1 - u/u_{\text{sing}}) + \dots) \quad (5.4)$$

where A'_{sing} and γ'_{sing} denote, respectively, the critical amplitude and the corresponding critical exponent, and the \dots represent analytic confluent corrections. One may observe that we have not included non-analytic confluent corrections to the scaling form in equation (5.4). The reason is that, as discussed in our earlier work [20], previous studies have indicated that they are very weak or absent for the 2D Ising model. We proceed to our results.

5.2. Singularity at $u = u_e$

We obtained the most accurate results using differential approximants. In table 2 we list the pole positions u_{sing} and corresponding exponents γ'_e for the approximants which yield poles closest to u_e †.

The dlog Padé approximants (PAs) gave similar, but slightly less accurate, results. For example, the [9/9] and [10/10] PAs yielded pole positions with normalized distances $|u_{\text{sing}} - u_e|/|u_e| = 3.2 \times 10^{-5}$ and 1.7×10^{-5} , and corresponding exponents $\gamma'_e = 1.2463$ and 1.2471, respectively. From this analysis, we infer the location of the singularity to be

$$u_{\text{sing}} = -0.17157 \pm 0.00001. \quad (5.5)$$

This, together with our knowledge of the exact location of the endpoint of the singular line segment (2.33), supports the conclusion that the exact location of this singularity is at $u = u_e = -0.1715729\dots$ given in (2.34). Accepting this conclusion, we plot the values of the corresponding exponent γ'_e for the differential approximants as functions of the normalized distance from this point, i.e. $|u_{\text{sing}} - u_e|/|u_e|$, and extrapolate to zero distance. (This extrapolation method is similar to the use of biased differential approximants; in both of these approaches, one uses one's knowledge of the exact position of the singularity.) From our extrapolation, we obtain

$$\gamma'_e = 1.25 \pm 0.01 \quad (5.6)$$

(where the quoted uncertainty reflects the scatter in the points and the estimated uncertainty from the small extrapolation to zero distance). This strongly supports the following inference for the exact value of this exponent, which we shall make

$$\gamma'_e = \frac{5}{4}. \quad (5.7)$$

To calculate the critical amplitude for $\bar{\chi}$ at the $u = u_e$ singularity, we use the standard method of analysing Padé approximants to the series $(-\bar{\chi}_r)^{1/\gamma'_e}$ (where the minus sign is

† To save space, we omit a number of tables of differential and Padé approximants. The reader may obtain these tables from the file `hep-lat/9412105`, archived at `hep-lat@xxx.lanl.gov` or directly from the authors.

Table 2. Values of pole near $u_c = -(3 - 2^{3/2}) = -0.171\,572\,876\dots$, normalized distance from this point, $|u_{\text{sing}} - u_c|/|u_c|$, and exponent γ'_c from differential approximants (DAs) to low-temperature series for $\bar{\chi}_r$. We list only the DAs which satisfy the accuracy criterion $|u_{\text{sing}} - u_c|/|u_c| \leq 2 \times 10^{-5}$.

$[L/M_0; M_1]$	u_{sing}	$ u_{\text{sing}} - u_c / u_c $	γ'_c
[0/5; 5]	-0.171 5743	0.81×10^{-5}	1.2474
[0/5; 6]	-0.171 5716	0.72×10^{-5}	1.2470
[0/5; 7]	-0.171 5696	1.9×10^{-5}	1.2467
[0/6; 5]	-0.171 5717	0.66×10^{-5}	1.2470
[0/7; 5]	-0.171 5706	1.3×10^{-5}	1.2469
[0/9; 9]	-0.171 5754	1.5×10^{-5}	1.2505
[0/9; 10]	-0.171 5716	0.72×10^{-5}	1.2481
[0/10; 9]	-0.171 5718	0.64×10^{-5}	1.2482
[1/7; 9]	-0.171 5702	1.6×10^{-5}	1.2475
[1/8; 9]	-0.171 5700	1.7×10^{-5}	1.2474
[1/8; 10]	-0.171 5701	1.6×10^{-5}	1.2475
[1/9; 8]	-0.171 5699	1.7×10^{-5}	1.2474
[1/9; 9]	-0.171 5704	1.4×10^{-5}	1.2476
[1/10; 8]	-0.171 5702	1.5×10^{-5}	1.2475
[2/7; 7]	-0.171 5701	1.6×10^{-5}	1.2463
[2/7; 9]	-0.171 5698	1.8×10^{-5}	1.2473
[2/8; 9]	-0.171 5737	0.45×10^{-5}	1.2501
[3/7; 8]	-0.171 5699	1.7×10^{-5}	1.2478
[3/7; 9]	-0.171 5697	1.9×10^{-5}	1.2464
[3/8; 7]	-0.171 5696	1.9×10^{-5}	1.2474
[5/5; 6]	-0.171 5754	1.4×10^{-5}	1.2488
[5/7; 5]	-0.171 5698	1.8×10^{-5}	1.2478
[5/8; 6]	-0.171 5723	0.35×10^{-5}	1.2495
[6/5; 5]	-0.171 5697	1.9×10^{-5}	1.2464
[6/7; 6]	-0.171 5746	0.99×10^{-5}	1.2505
[7/4; 6]	-0.171 5707	1.3×10^{-5}	1.2495
[7/5; 7]	-0.171 5709	1.2×10^{-5}	1.2483
[8/6; 4]	-0.171 5700	1.7×10^{-5}	1.2476
[9/6; 4]	-0.171 5709	1.1×10^{-5}	1.2483
[10/5; 3]	-0.171 5698	1.8×10^{-5}	1.2476
[11/5; 3]	-0.171 5707	1.2×10^{-5}	1.2481

inserted because $c_0 = -1$ in equation (5.2)). For A'_e as defined in equation (5.4) with $u_{\text{sing}} = u_c$, we obtain

$$A'_e = -0.115\,15 \pm 0.000\,20. \tag{5.8}$$

5.3. Singularity at $u = 1$

Our most precise results for $\bar{\chi}_r$ relevant to the singularity at $u = 1$ are again from differential approximants; we list a few of these in table 3.

The dlog Padé approximants yield similar values. From these results, we obtain the location of the singularity as

$$u_{\text{sing}} = 0.999 \pm 0.001. \tag{5.9}$$

From this and our determination of the phase boundaries (2.32)–(2.33), we infer that the exact location of this singularity is at $u = 1$. Given this conclusion, we then plot the values

Table 3. Values of pole near $u = 1$, normalized distance from this point, $|u_{\text{sing}} - 1|$, and exponent γ'_1 from differential approximants to low-temperature series for $\bar{\chi}_r$. We list only the differential approximants which satisfy the accuracy criterion $|u_{\text{sing}} - 1| \leq 1 \times 10^{-3}$.

$[L/M_0; M_1]$	u_{sing}	$ u_{\text{sing}} - 1 $	γ'_1
[0/9; 9]	0.999 9105	0.89×10^{-4}	2.4776
[1/6; 8]	0.998 9524	1.0×10^{-3}	2.4554
[1/9; 9]	0.999 0590	0.94×10^{-3}	2.4617
[2/4; 6]	1.000 4562	0.46×10^{-3}	2.4545
[2/6; 4]	1.000 8071	0.81×10^{-3}	2.4534
[2/6; 7]	0.999 7299	2.7×10^{-4}	2.4678
[2/7; 6]	0.999 6006	4.0×10^{-4}	2.4651
[2/8; 8]	1.000 6495	0.65×10^{-3}	2.4969
[3/6; 6]	1.000 5153	0.52×10^{-3}	2.4841
[3/9; 7]	0.999 1902	0.81×10^{-3}	2.4621
[4/7; 8]	0.999 0659	0.93×10^{-3}	2.4624
[4/8; 7]	0.999 0450	0.96×10^{-3}	2.4618
[5/4; 5]	1.000 9762	0.98×10^{-3}	2.4429
[5/6; 7]	0.999 3881	0.61×10^{-3}	2.4709
[5/6; 8]	0.999 1317	0.87×10^{-3}	2.4644
[5/7; 7]	0.999 0811	0.92×10^{-3}	2.4629
[5/8; 6]	1.000 0180	1.8×10^{-5}	2.4888
[6/4; 6]	0.999 3653	0.63×10^{-3}	2.5040
[6/5; 7]	1.000 2641	2.6×10^{-4}	2.4944
[6/6; 7]	0.999 1189	0.88×10^{-3}	2.4641
[6/7; 5]	1.000 3178	3.2×10^{-4}	2.4956
[6/7; 6]	0.999 3080	0.69×10^{-3}	2.4698
[7/5; 6]	0.999 0014	1.0×10^{-3}	2.4565
[8/4; 6]	0.999 3253	0.67×10^{-3}	2.4757
[8/5; 6]	0.999 4784	0.52×10^{-3}	2.4852

of γ'_1 as a function of the distance from $u = 1$ and extrapolate to zero distance. This yields the value

$$\gamma'_1 = 2.50 \pm 0.01 \quad (5.10)$$

(where, as before, the quoted uncertainty reflects the scatter in the points and the estimated uncertainty from the small extrapolation to zero distance). This strongly supports the following inference that we shall make for the exact value of this exponent

$$\gamma'_1 = \frac{5}{2}. \quad (5.11)$$

Hence, in particular,

$$\gamma'_1 = 2\gamma'_e. \quad (5.12)$$

We note that the relation (5.12) can be understood if one re-expresses $\bar{\chi}$ as a function of the elliptic modulus variable $k_<$ in equation (2.7), since $k_<$ diverges at $u = 1$ with an exponent which is twice as large as the exponent describing its divergence at $u = u_e$, i.e., $k_< \sim (1 - u)^{-1}$ as $u \rightarrow 1$, while $k_< \sim (1 - u/u_e)^{-1/2}$ as $u \rightarrow u_e$.

5.4. Singularity at $u = -1$

We have studied the singularity in $\bar{\chi}$ at $u = -1$ (denoted u_s) by using the series for $\bar{\chi}$ in the variable u and also transforming this series to one in the elliptic modulus variable $k_<$. The series in $k_<$ showed a greater sensitivity to this singularity, and therefore we concentrate on

the results from our analysis of this series. The reason for this greater sensitivity is clear; the series in u is strongly affected by the fact that, as one can see from figure 2(a), there is an intervening singular line segment protruding into the FM phase and ending at $u = u_e$, in front of the point $u = -1$ as one moves out from the origin along the negative $\text{Re}(u)$ axis. The transformation from u to $k_<$ maps the singular endpoint at $u = u_e$ away to $-\infty$ and maps the singularity at $u = 1$ to ∞ in the $k_<$ plane, thereby leaving the singularity at $u = -1$ as the nearest to the origin. Specifically, the image of the singular line segment from $u = u_e$ leftward to $u = -1$ is the semi-infinite line segment from $-\infty$ to -1 in the $k_<$ plane. The line segment from $u = 1/u_e$ to $u = -1$ has the same image, again the segment from $-\infty$ to -1 in the $k_<$ plane, while the unit circle $|u| = 1$ maps to the line segment from one to ∞ in this plane. The series in $k_<$ has the form $\bar{\chi} = (1/4)(k_<)^2 \sum_{n=0}^{\infty} c'_n(k_<)^n$, and, as before, we actually analyse the reduced function $\bar{\chi}_r = 4(k_<)^{-2}\bar{\chi}$.

Using the Taylor series expansion of $k_<$ near $u = -1$

$$k_< = -1 - 2^{-5}(1+u)^4 + O((1+u)^5) \quad (5.13)$$

it follows that as $k_< \rightarrow -1$ and $u \rightarrow -1$, the singular form $\bar{\chi} \sim (1+k_<)^{-\gamma'_{s,k_<}}$ corresponds to $\bar{\chi} \sim (1+u)^{-\gamma'_s}$, with

$$\gamma'_s = 4\gamma'_{s,k_<}. \quad (5.14)$$

Because the actual pole positions in the differential approximants have small imaginary parts, typically a few times 10^{-4} of the size of the real part, there are resultant imaginary parts in the values of the corresponding exponent γ'_s from the differential approximants. Since the exact singularity in $\bar{\chi}(u)$ is at the real value $u = -1$, and since $\bar{\chi}(u, h = i\pi/2)$ is real for real u , we know that γ'_s at $u = (k_<) = -1$ is real. Given this and the relation (5.14), it follows that we may take only the real parts of the exponents from the differential approximants to the series in $k_<$, and we do so. From this study, we obtain for the position of the singularity

$$(k_<)_{\text{sing}} = -0.9993 \pm 0.0001 \quad (5.15)$$

consistent with the expectation $(k_<)_{\text{sing}} = -1$, or equivalently, $u_{\text{sing}} = u_s = -1$. The values of $\text{Re}(\gamma'_s)$ from the differential approximants are almost all slightly below 0.25; however, when we carry out our method of plotting the values as a function of the distance $|(k_<) + 1|$ and extrapolating to zero distance from the exact singularity, the extrapolated value is actually slightly above 0.25. Accordingly, we give a conservative estimate

$$\gamma'_{s,k_<} = 0.250 \pm 0.020 \quad (5.16)$$

and hence, using (5.14),

$$\gamma'_s = 1.00 \pm 0.08. \quad (5.17)$$

This supports the conclusion, which we shall draw, that the exact value of this exponent is

$$\gamma'_s = 1. \quad (5.18)$$

We show our summary of exponents in table 4. The exponent relation $\alpha'_{u,\text{ph}} + 2\beta'_u + \gamma'_{u,\text{ph}} = 2$ is evidently satisfied at all three of the singularities $u = u_e$, $u = 1$ and $u = -1$.

6. Extraction and analysis of low-temperature series for $\bar{\chi}^{(a)}$

We have also investigated the complex-temperature singularities in the staggered susceptibility $\bar{\chi}^{(a)}$ for the present model. To do this, we have extracted and analysed the low-temperature series expansion for this function, using the low-temperature, high staggered

Table 4. Exponents at singularities in the 2D Ising model with $h = \pm i\pi/2$. The results for α'_u and β_u are exact; the results for γ'_u are our conclusions for the exact values from our series analysis. The notation — indicates that the point cannot be approached from within the given phase. For the singularity of C at $u = 1$ (marked with a *), the values of α' correspond to evaluating $K = -(1/4)\ln(1) = 0$ on the principal Riemann sheet of the logarithm, as discussed in the text.

u	$\alpha'_{u,\text{FM}}$	$\alpha'_{u,\text{AFM}}$	β_u	γ'_u	$\alpha'_{u,\text{ph}} + 2\beta'_u + \gamma'_{u,\text{ph}}$
$u_e = -(3 - 2^{3/2})$	1	—	-1/8	5/4	2
1	0 finite*	0 finite*	-1/4	5/2	2
$u_c = -1$	0 finite	0 finite	1/2	1	2

field series expansions for the free energy of the Ising model on the square lattice calculated by the King's College group [31, 26]. These are denoted antiferromagnetic polynomials in these papers and were calculated to order $O(w^{11})$ in [26], where, as before, $w = 1/u$ is the low-temperature expansion variable in the AFM phase. The antiferromagnetic polynomials were apparently not calculated to higher order subsequently [32].

We have extracted from these the resultant low-temperature series expansion for $\bar{\chi}^{(a)}$ for $h = i\pi/2$, which is

$$\bar{\chi}^{(a)}(h = i\pi/2) = 4w^2[-1 - 8w^2 + 24w^3 - 135w^4 + 648w^5 - 3336w^6 + 17\,240w^7 - 90\,501w^8 + 479\,192w^9 + O(w^{10})]. \quad (6.1)$$

For reference, we recall that the series for $\bar{\chi}^{(a)}$ for $h = 0$ on this lattice is [31, 26]

$$\bar{\chi}^{(a)}(h = 0) = 4w^2[1 + 4w^2 + 8w^3 + 39w^4 + 152w^5 + 672w^6 + 3016w^7 + 13\,989w^8 + 66\,664w^9 + O(w^{10})]. \quad (6.2)$$

The series (6.1) is much shorter than the one which we extracted for $\bar{\chi}$, given by equation (5.2) and table 1, and hence one does not expect to derive results for $\bar{\chi}^{(a)}$ which are as precise as those which we obtained for $\bar{\chi}$. As before, we have used both dlog Padé and differential approximants for this analysis.

We study first the vicinity of the singular point $w = 1$, using Padé and differential approximants. One would not normally expect a dlog Padé approximant of such low order as [1/2] to yield an accurate result; however, it happens that the denominator of this approximant is $\propto (1-w)(1-(11/2)w)$, so that it produces a location for the pole which is exact. For this reason, it yields a much better determination of the associated exponent than would otherwise have been the case; this is $\gamma'_{1,a} = 2.462$. The differential approximant which locates the pole position most accurately is the [2/2;2] DA, yielding $w_{\text{sing}} = 0.999\,046$ and $\gamma'_{1,a} = 2.554$. From the full set of Padé and differential approximants we infer the crude result

$$\gamma'_{1,a} = 2.5 \pm 0.5 \quad (6.3)$$

where the quoted uncertainty reflects the scatter in the values obtained from the various PA and DA approximants. This is consistent with the exact value $\gamma'_{1,a} = 5/2$ and hence with the equality $\gamma'_{1,a} = \gamma'_1$. However, clearly the results for $\gamma'_{1,a}$ are much less precise than our determination of γ'_1 .

We also studied the series in the vicinity of the singular endpoint $w = w_e = -(3 - 2^{3/2})$ (i.e. $u = u_{0e} = 1/u_e = -(3 + 2^{3/2})$). To optimize the sensitivity, we calculated and analysed series in transformed variables to map the singularity at $w = 1$ away. We required these variables to be equal to w for small w and to map $w = \pm\infty$ to $\pm\infty$, respectively. Two

such variables were $w' = w(1 + w/8)(1 - w)^{-1}$ and $w'' = w(1 - w)^{-1} \sinh w$. The series in the transformed variables did slightly better in locating the pole positions in w'_e and w''_e corresponding to w_e . The dlog Padé and differential approximants indicated that $\bar{\chi}^{(w)}$ has a divergent singularity at w_e and yielded values for the associated exponent $\gamma'_{oc,a}$ in the range from about 0.2 to 0.4. Given our exact results $\alpha'_{oc} = 1$ for the specific heat and $\beta_{oc} = -1/4$ for the staggered magnetization, a value within the above range for $\gamma'_{oc,a}$ would indicate a violation of the exponent relation $\alpha'_{oc} + 2\beta_{oc} + \gamma'_{oc} = 2$. In this context, it is of interest to note that we have already found violations of the relation $\alpha + 2\beta + \gamma = 2$ at complex-temperature singularities, e.g. in the zero-field Ising model on the square lattice at $u \approx u_s = -1$, as approached from within the PM phase, where $\alpha_s = 0$, $\beta_s = 1/4$ and $\gamma_s < 0$ (since $\bar{\chi}$ has a finite non-analyticity for the approach from within the PM phase) [20], and in the zero-field Ising model on the honeycomb lattice, at the point $z = z_\ell = -1$, as approached from within the FM phase, where $\alpha'_\ell = 2$, $\beta'_\ell = -1/4$ and $\gamma'_\ell = 5/2$, so that $\alpha'_\ell + 2\beta'_\ell + \gamma'_\ell = 4$ [21].

7. Complex-temperature behaviour of the correlation length

In this section we shall study the complex-temperature behaviour of the correlation length. To do this, we make use of a calculation of the asymptotic form of the spin-spin correlation function along a row (or equivalently, column), $\langle \sigma_{0,0} \sigma_{n,0} \rangle$, for large n [5] (where, without loss of generality, one may take $n > 0$). From this calculation, carrying out an analytic continuation to complex temperature, we obtain, for $n \rightarrow \infty$,

$$\begin{aligned} \langle \sigma_{0,0} \sigma_{n,0} \rangle_{\text{conn}} &\sim -(2/\pi)(1 - u^2)^{-1} M^2 n^{-1} u(-u)^n \\ &= -(2/\pi)(1 - u)^{-3/2} (1 + 6u + u^2)^{-1/4} n^{-1} u(-u)^n \end{aligned} \quad (7.1)$$

where we have used the exact expression for M , (4.1). This analytic continuation applies within the FM phase. Extracting the correlation length ξ in the usual way as $\xi^{-1} = -\lim_{r \rightarrow \infty} r^{-1} \ln(\langle \sigma_0 \sigma_r \rangle_{\text{conn}})$, where $r \equiv |r|$, we find

$$\xi_{\text{row}}^{-1} = -\ln(-u). \quad (7.2)$$

For usual physical second-order critical points, one can use the connected two-spin correlation function for any r , with $|r| \rightarrow \infty$, to extract the correlation length ξ . However, in our previous work [19, 20], we found that at the complex-temperature singular point $u = u_s = -1$ in the zero-field Ising model on the square lattice, the correlation length defined from the diagonal connected two-spin correlation function diverges with a different exponent, $\nu'_{s,\text{diag}} = 2$, from the exponent $\nu'_s = 1$ describing the divergence in the correlation length defined from off-diagonal (e.g. row) correlation functions. In view of this, we include the suffix row in (7.2) for clarity. We now consider three particular singular points which can be approached from within the complex-temperature FM phase, viz., $u = u_e$, $u = -1$ and $u = 1$. As $u \rightarrow u_e$, the two-spin correlation function (7.1) diverges, as $(1 - u/u_e)^{-1/4}$, because of the divergence in the prefactor M^2 , but the correlation length ξ_{row} remains finite, with $\xi_{\text{row}}^{-1} = -\ln(-u_e) = 1.7627 \dots$ at $u = u_e$. If this feature of a finite correlation length applied to all of the connected two-spin correlation functions, precisely at $u = u_e$ as well as for points approaching u_e from within the complex-temperature FM phase, then by the same argument as was used in [8], it would follow that the only singularity in $\bar{\chi}$ would arise from the divergent M^2 prefactor†. We know, however, that the above premise cannot be

† Define $\langle \sigma_0 \sigma_r \rangle = M^2 c(r)$. Then $\bar{\chi} = M^2 \sum_r c(r)$. For purposes of analysing divergences, the asymptotic behaviour of the sum can be approximated by that of the integral $\int d^2r c(r)$ for large r (with a short-distance

true, since then the susceptibility exponent at u_e (as approached from within the FM phase) would be $1/4$, whereas we found that $\gamma'_e = 5/4$. The fact that the susceptibility diverges with an exponent different from that arising from the divergent M^2 prefactor shows that at least some connected two-spin correlation functions must decay like a power law, i.e. the associated correlation length must be divergent, at $u = u_e$. To obtain more information on this, it would be useful to carry out analytic calculations of the asymptotic forms of the general two-spin correlation functions $\langle \sigma_{0,0} \sigma_{m,n} \rangle$ in the present model, near to and at this singular point.

As $u \rightarrow 1$, the two-spin correlation function (7.1) again diverges, as $(1 - u)^{-3/2}$, and the correlation length ξ_{row} is finite: $\xi_{\text{row}}^{-1} = -\ln(-1) = -i\pi$ (for the principal Riemann sheet of the logarithm). This is a case similar to that discussed in [8] where $\text{Re}(\xi^{-1}) = 0$ but $\text{Im}(\xi^{-1}) \neq 0$.

As $u \rightarrow -1$, each two-spin correlation function is finite, but the correlation length does diverge, with exponent

$$\nu'_s = 1. \tag{7.3}$$

If one were to use the exponent relation $\gamma'_s = \nu'_s(2 - \eta_s)$, then with our inference $\gamma'_s = 1$ in equation (5.18), it would follow that $\eta_s = 1$. However, we have shown previously [20] that one must use caution in trying to apply such exponent relations at complex-temperature singularities, since different connected spin-spin correlation functions may be characterized by correlation lengths which diverge with different exponents ν .

This type of analysis can also be done with the staggered two-spin correlation functions (cf (4.11))

$$\langle \tilde{\sigma}_{0,0} \tilde{\sigma}_{n,0} \rangle_{\text{conn}} = (-1)^n \langle \sigma_{0,0} \sigma_{n,0} \rangle_{\text{conn}}. \tag{7.4}$$

In particular, as $u \rightarrow 1/u_e$ (i.e. $w \rightarrow w_e$), these correlation functions diverge, as $(1 - w/w_e)^{-1/4}$, because of the divergent prefactor M_{st}^2 . However, the correlation length $\xi_{\text{row,AFM}}$ remains finite. If this behaviour characterized all of the staggered two-spin correlation functions, at w_e as well as in the vicinity of w_e , then the only divergence in $\bar{\chi}^{(a)}$ would arise from the M_{st}^2 prefactor, and hence $\gamma'_{e,a} = 1/4$. This value is consistent with our results from the analysis of the low-temperature series for $\bar{\chi}^{(a)}$. This merits further study.

8. Exact solution at $u = 1$ for arbitrary H

In the body of this paper, we have investigated singularities in the square lattice Ising model as functions of complex temperature, for the fixed value of external magnetic field, $h = i\pi/2$ (or $h = -i\pi/2$). It is also of interest to study the complementary problem of singularities as a function of h for fixed K or u . Indeed, in pursuing such a study, Yang and Lee were led to their celebrated circle theorem on the zeros of the partition function for the Ising model in the complex e^{2h} plane [3,33]. Here, we would like to mention some elementary results which elucidate how various quantities become singular at a particularly simple point, $u = 1$, as h is varied. These results may be combined with our determination of the exact singularities in f , U , C and M as one approaches this point by varying u . At $J = 0$, hence $K = 0$ and $u = 1$, the partition function reduces to a single-site problem, which can easily be calculated exactly for arbitrary H , dimensionality and lattice type. We

cutoff on the latter). If $c(r) \sim r^{-p} e^{-r/k}$ as $r \rightarrow \infty$, this integral is finite. Therefore, a divergence in $\bar{\chi}$ would arise solely from a divergence in the prefactor M^2 . This was noted in [20].

find, independent of the dimensionality and lattice type

$$f(u = 1, h) = \ln(2 \cosh h) \tag{8.1}$$

$$U = -H \tanh h \tag{8.2}$$

$$k_B^{-1} C = \frac{h^2}{\cosh^2 h} \tag{8.3}$$

$$M = \tanh h \tag{8.4}$$

$$\tilde{\chi} = \frac{1}{\cosh^2 h}. \tag{8.5}$$

Further, the m -point correlation functions factorize trivially and are independent of the positions of the spins

$$\langle \sigma_{r_1} \dots \sigma_{r_m} \rangle = \langle \sigma_{r_1} \rangle^m = M^m = (\tanh h)^m. \tag{8.6}$$

To study the singularities of these functions, we must define new exponents, since the usual critical exponents apply to singularities of thermodynamic quantities as functions of T . To avoid a profusion of new symbols, we shall use the same Greek letters as for the respective T -dependent singularities in thermodynamic quantities, but use a superscript (h) to indicate that they describe the singularity as a function of h for $K = 0$. Thus, for the leading singularity in the specific heat, as a function of h , at the point $h = h_s$ (s denotes a generic singularity here) for fixed $K = 0$ (hence $u = 1$), we shall write

$$C(h)_{\text{sing}} \sim A_{C,s,\text{dir}}^{(h)} (h - h_s)^{-\alpha_{s,\text{dir}}^{(h)}} \tag{8.7}$$

where dir denotes the direction, in the complex h plane, from which one approaches the singular point h_s . Similarly, we shall write

$$\chi_{\text{sing}} \sim A_{\chi,s,\text{dir}}^{(h)} (h - h_s)^{-\nu_{s,\text{dir}}^{(h)}} \tag{8.8}$$

and so forth for the singularities in other quantities. From (8.3), it is evident that C diverges for

$$h = (2n + 1) \frac{i\pi}{2} \quad n \in \mathbb{Z} \tag{8.9}$$

with corresponding exponent $\alpha_1^{(h)} = 2$ for any direction of approach to any of the singular points (8.9). The internal energy itself also diverges at these points, with the exponent $\alpha_1^{(h)} - 1 = 1$ and vanishes at the set

$$h = n i \pi \quad n \in \mathbb{Z}. \tag{8.10}$$

The magnetization vanishes and diverges at the same set of points as the internal energy U (cf equations (8.10) and (8.9)) with the respective exponents $\beta_{1,\text{zero}}^{(h)} = 1$ and $\beta_{1,\text{div}}^{(h)} = -1$, again, independent of the direction of approach to these points in the complex h plane. The susceptibility diverges at the points (8.9) with exponent $\gamma_1^{(h)} = 2$.

It is useful to evaluate the general results above for the interesting special case of complex $h = h_r + i\pi/2$, where h_r is real. For this case, we have $f = \ln(2i \sinh h_r)$, $U = -H / \tanh h_r$, $k_B^{-1} C = -(h_r + i\pi/2)^2 / \sinh^2 h_r$, $M = 1 / \tanh h_r$, $\tilde{\chi} = -1 / \sinh^2 h_r$ and $\langle \sigma_{r_1} \dots \sigma_{r_m} \rangle = (\tanh h_r)^{-m}$. As $h_r \rightarrow 0$ so that $h \rightarrow i\pi/2$, we recover our previous results, that U and M diverge linearly while C and $\tilde{\chi}$ diverge quadratically.

For loose-packed lattices, it is straightforward to extend these results to consider a staggered rather than uniform external field, H_{st} , i.e. to consider the partition function $Z = \sum_{\{\sigma_n\}} \exp(\sum_n (-1)^{p(n)} h_{\text{st}} \sigma_n)$, where $p(n)$ was defined in equation (4.12) and $h_{\text{st}} = \beta H_{\text{st}}$. Since the summations over the spins on the even and odd sublattices are

decoupled, one finds the same equations as before, but with H replaced by H_{st} , i.e. $f = \ln(2 \cosh h_{st})$, $U = -H_{st} \tanh h_{st}$, $C = k_B h_{st}^2 / \cosh^2 h_{st}$ and $M_{st} = \tanh h_{st}$. The staggered susceptibility is $\bar{\chi}^{(a)} = 1 / \cosh^2 h_{st}$.

9. Conclusions

In this paper, we have studied a natural generalization of an exactly solved model from real non-negative temperature to complex temperature. This is the Ising model on the square lattice in an external magnetic field given by $\beta H = \pm i\pi/2$, first solved by Lee and Yang [3]. We have worked out the complex-temperature phase boundaries, as shown in figure 2. We have also extracted a low-temperature series expansion for the susceptibility, $\bar{\chi}$. From an analysis of this series using dlog Padé and differential approximants, we conclude that $\bar{\chi}$ has divergent singularities at $u = u_e = -(3 - 2^{3/2})$ with exponent $\gamma'_e = 5/4$, at $u = 1$ with exponent $\gamma'_1 = 5/2$ and at $u = u_s = -1$ with exponent $\gamma'_s = 1$. We have also studied the staggered susceptibility. Using exact results, we have determined the complex-temperature singularities of the specific heat and the uniform and staggered magnetization. We are currently in the process of extending our studies to other 2D lattices. The findings show again that even though the Ising model has a very simple Hamiltonian, it exhibits a fascinating richness of properties.

Acknowledgments

This research was supported in part by the NSF grant PHY-93-09888. One of us (RS) thanks Professor C N Yang for a discussion of [3] and Professors D S Gaunt and A J Guttmann for discussions of the current status of low-temperature series expansions.

References

- [1] Onsager L 1944 *Phys. Rev.* **65** 117
- [2] Yang C N 1952 *Phys. Rev.* **85** 808
- [3] Lee T D and Yang C N 1952 *Phys. Rev.* **87** 410
- [4] Baxter G 1965 *J. Math. Phys.* **6** 1015; 1966 *J. Math. Phys.* **8** 399
- [5] McCoy B and Wu T T 1967 *Phys. Rev.* **155** 438
- [6] Merlini D 1974 *Lett. Nuovo Cim.* **9** 100
- [7] Lin K Y and Wu F Y 1988 *Int. J. Mod. Phys. B* **4** 471
- [8] Marchesini G and Shrock R E 1989 *Nucl. Phys. B* **318** 541
- [9] Utiyama T 1951 *Prog. Theor. Phys.* **6** 907
- [10] Syozi I and Naya S 1960 *Prog. Theor. Phys.* **23** 374; 1960 *Prog. Theor. Phys.* **24** 829
- [11] Baxter R J 1986 *Proc. R. Soc. A* **404** 1
- [12] Suzuki M 1991 *J. Phys. Soc. Japan* **60** 441
- [13] Fisher M E 1965 *Lectures in Theoretical Physics* vol 7C (Boulder, CO: University of Colorado) p 1
- [14] Katsura S 1967 *Prog. Theor. Phys.* **38** 1415
Abe Y and Katsura S 1970 *Prog. Theor. Phys.* **43** 1402
- [15] Ono S, Karaki Y, Suzuki M and Kawabata C 1968 *J. Phys. Soc. Japan* **25** 54
- [16] Thompson C J, Guttmann A J and Ninham B W 1969 *J. Phys. C: Solid State Phys.* **2** 1889
Guttmann A J 1969 *J. Phys. C: Solid State Phys.* **2** 1900
- [17] Domb C and Guttmann A J 1970 *J. Phys. C: Solid State Phys.* **3** 1652
- [18] Guttmann A J 1975 *J. Phys. A: Math. Gen.* **8** 1236
- [19] Enting I G, Guttmann A J and Jensen I 1994 *J. Phys. A: Math. Gen.* **27** 6963
- [20] Matveev V and Shrock R 1995 *J. Phys. A: Math. Gen.* **28** 1557
- [21] Matveev V and Shrock R Complex-temperature singularities in the $d = 2$ Ising model: triangular and honeycomb lattices *J. Phys. A: Math. Gen.* in press

- [22] Gradshteyn I and Ryzhik I 1980 *Table of Integrals, Series and Products* (New York: Academic)
- [23] Kaufmann B and Onsager L 1949 *Phys. Rev.* **76** 1244
- [24] Montroll E W, Potts R B and Ward J C 1963 *J. Math. Phys.* **4** 308
- [25] Ghosh R K and Shrock R E 1984 *Phys. Rev. B* **30** 3790, 1985 *J. Stat. Phys.* **38** 473, 1985 *Phys. Rev. B* **31** 1486
- [26] Sykes M F, Gaunt D S, Martin J L, Mattingly S R and Essam J W 1973 *J. Phys. A: Math. Gen.* **14** 1071
- [27] Sykes M F, Watts M G and Gaunt D S 1975 *J. Phys. A: Math. Gen.* **8** 1448
- [28] Baxter R J and Enting I G 1979 *J. Stat. Phys.* **21** 103
- [29] Briggs K M, Enting I G and Guttman A J 1994 *J. Phys. A: Math. Gen.* **27** 1503
- [30] Guttman A J 1989 *Phase Transitions and Critical Phenomena* vol 13, ed C Domb and J Lebowitz (New York: Academic)
- [31] Sykes M F, Essam J W and Gaunt D S 1965 *J. Math. Phys.* **6** 283 and references therein
- [32] Gaunt D S 1994 private communication
- [33] Yang C N and Lee T D 1952 *Phys. Rev.* **87** 404